Nanofabrication (2022) 7, 104-115
https://doi.org/10.37819/nanofab.007.200

RESEARCH ARTICLE

Studies on high performance rubber composites by incorporating titanium dioxide particles with different surface area and particle size

Vineet Kumara*, Anuj Kumar[b], Rajesh K. Chhatra[c], and Dong-Joo Lee[a]

[a]*School of Mechanical Engineering, Yeungnam University, 280 Daehak-ro, Gyeongsan 38541, South Korea.*
[b]*School of Chemical Engineering, Yeungnam University, 280 Daehak-ro, Gyeongsan 38541, South Korea.*
[c]*Department of Chemistry, Indian Institute of Technology Delhi, New Delhi 110016, India.*
**Corresponding author email: vineetfri@gmail.com*

ABSTRACT

In this work, we incorporate titanium dioxide (TiO_2) particles as fillers into room temperature vulcanized silicone rubber (RTV-SR) and fabricated the RTV-SR/TiO_2 composites. Herein, the effect of various surface areas of TiO_2 particles on the mechanical properties of RTV-SR/TiO_2 composites was investigated. The particle size of different types of TiO_2 particles (147 nm, 34 nm, and 29 nm) was measured by using scanning electron microscopy (SEM), whereas the Brunauer–Emmett–Teller (BET) surface area was measured through adsorption-desorption isotherms as 3, 50, and 145 m^2/g, respectively. TiO_2 particles reinforced RTV-SR composites were prepared by solution mixing method. TiO_2 particles with smaller particle sizes and high BET surface area exhibited higher mechanical properties. The compressive moduli were obtained as 2.2 MPa for a virgin sample and increased to 2.6 MPa, 2.8 MPa and 3.24 MPa for 3, 50, and 145 m^2/g samples respectively at 6 phr filler loading. Similarly, the fracture strain of the composite was 117% for a virgin sample and changed to 94%, 130%, and 205% for 3, 50, and 145 m^2/g samples, respectively, at 8 phr filler loading. The surface area and particle size of the fillers showed significant effect on mechanical properties of the composites, but no significant effect was observed on the energy harvesting values of RTV-SR/TiO_2 composites.

ARTICLE HISTORY

Received: 18-05-2022
Revised: 17-06-2022
Accepted: 20-06-2022

KEYWORDS

Titanium dioxide;
Silicone rubber,
BET surface area;
Particle size;
Mechanical property;
Energy harvesting

1. Introduction

There is an increasing energy demand after the industrialization of mankind. In last century, the energy demand has been fulfilled though non-renewable sources such as coal or petroleum. But these sources are limited and lead to several challenges, such as global warming. Due to global warming, the world has been forced to switch towards green energy and renewable sources. Lab lab-scale energy generation has recently been demonstrated using conductive rubber composites [1]. The energy outcome from the composites is obtained by harvesting mechanical motions into few millivolts. These devices for energy harvesting are straightforward, easy to prepare, and process and useful renewable energy sources [2]. Further, the rubber reinforced with the conductive filler is a source of electrode sandwiched and separated by a dielectric elastomer slab (silicone rubber) [3]. Under external mechanical forces (e.g., mechanical compressive or tensile stress), the device undergoes deformation (i.e. strain) and thereby it generates the electrical energy from the mechanical energy. This phenomenon is known as piezo-electric effect [4].

The variation in particle size, surface area, and morphology of the fillers has a significant effect on the composite materials' characteristics [5, 6]. Among them, the particle size of the filler acts as a key feature in affecting the properties remarkably [7]. Also, the fillers of smaller particle size with higher surface area promote greater interfacial interaction with the polymer chains of the rubber matrix. Herein, polymeric chains are adsorbed on filer surfaces owing to their high surface energy. Therefore, the fillers with higher surface area promote more polymer chain adsorption on their surfaces and facilitate higher interfacial interaction [8]. Higher interfacial interaction promotes higher stress transfer effect between polymer and filler in the composite. Various nanofillers are recently used to reinforce rubber due to the raw rubber's poor mechanical properties and stickiness [9]. The reinforcing and conductive nanofillers not only improve the mechanical and electrical properties of the rubber but also make them useful for various applications, such as energy harvesting [10].

Among the nanofillers, graphene, carbon nanotube and recently titanium dioxide (TiO_2) has been widely utilized in rubber-based composites [11,12]. TiO_2 has been most promising herein due to its easy dispersion, spherical morphology and efficient filler networking. Few studies of using TiO_2 showed the efficiency of the filler when it was used in rubber matrix and led to the high performance of the composites [13,14]. The rubber can be categorized in various types, including natural, butadiene and silicone rubbers. Among them, silicone rubber (SR) has been most promising due to its easy processing, easy to cure, high performance and soft nature with Shore A hardness of below 65 [15]. The SR can be further categorized based on types of vulcanization temperatures such as high, low, and room temperature [16,17]. Among them, room temperature vulcanized SR is most promising due to its easy curing and high tensile mechanical strength. Using room temperature vulcanized silicone rubber is useful for various soft applications such as strain sensors, actuation, or energy harvesting [18,19].

Several studies have been reported involving the reinforcement of nanofillers into rubber matrices and improved the properties of the obtained composites [18, 20, 21]. However, few studies have been reported to involve TiO_2 as nanofiller in SR to enhance the composites' performance [14,22]. Also, some studies involved the use of TiO_2 for biological activities [23,24]. Furthermore, the use of TiO_2 with different particle size for energy harvesting applications has least been reported in literature. Therefore, the present work reports the effect of BET surface area or different particle sizes of TiO_2 as nanofillers on the properties of silicone rubber. The surface area and particle size of TiO_2 particles measured using Brunauer–Emmett–Teller (BET) adsorption-desorption isotherms and scanning electron microscopy (SEM), respectively. TiO_2 particles reinforced RTV-SR composites were prepared by the solution mixing method and characterized for structural, morphological, and mechanical analyses. The results showed that the particle size plays a crucial role in determining the properties of the composites, and the nanofiller with a high surface area was found to exhibit better performances.

2. Materials and Methods

2.1. Materials

RTV silicone rubber (RTV-SR) (KE441) was purchased from Shin-Etsu, Japan and used as a rubber matrix in present work. The curing agent (CAT-RM) was also obtained from Shin-Etsu, Japan. For RTV-SR composites, the fillers used were different types of titanium oxide (TiO_2) based on different BET surface area and different particle size. These fillers were micron sized TiO_2 (Puratronic) with BET surface area of 3 m^2/g or particle size of 147 nm and bought from Alfa Aesar. The nano-sized fillers were TiO_2 nanopowder bought from Alfa Aesar with BET surface area of 145 m^2/g or particle size of 29 nm, and another is TiO_2 nanopowder purchased from PlasmaChem GmbH, Berlin, Germany with BET surface area of 50 m^2/g or particle size of 34 nm.

2.2. Preparation of composites

The preparation of composites was optimized in previous work [25,26]. In this work, the sample preparation was initiated by spraying the sample mold with a mold releasing agent and kept for 2 hours at room temperature for drying. For the preparation of rubber composites, the various filler powder (different grades of TiO_2) were added to

Samples codes	RTV-SR (phr)	Surface area (m^2/g)	Particle size (nm)	TiO_2 content (phr)	Vulcanizing agent (phr)
RTV-SR	100	-	-	-	2
RTV-SR/TiO_2-3	100	3	147	2-10	2
RTV-SR/TiO_2-50	100	50	34	2-10	2
RTV-SR/TiO_2-145	100	145	29	2-10	2

Table 1. Details about formulations

different content (Table-1) in liquid RTV-SR and manually mixed for at least 10 min. After this step, 2 phr of hardener were added into a composite slurry and mixed for 1 minute, and the composites slurry was poured into the sprayed cylindrical and rectangular molds. The cylindrical mold samples were used for studying compressive mechanical properties, and rectangular molds were used for studying tensile mechanical properties. Finally, the molds were manually pressed and kept at 24 hours at room temperature for curing.

2.3. Characterization

The particle size and microstructure of the TiO_2 powder were determined by SEM (S-4100, Hitachi), equipped with EDX. XRD (D8 Advance, Bruker) was performed to investigate the crystalline state of the TiO_2 powder at a scan rate of 10^o/min. Adsorption isotherms were performed using BELSORP-max (BEL, Japan Inc.) at 77 K to estimate the BET surface area of TiO_2 powder. The dispersion of TiO_2 powder with different particle sizes, and different surface areas in RTV-SR was studied using optical microscopy (Sometech) at a resolution of 150x. The filler dispersion was further investigated using elemental mapping. The elemental mapping was performed using X-ray mapping, SEM/EDX (Horiba, E_{max}, Tokyo, Japan). The procedure of sample preparation and measurements was described in our previous work [14]. Static mechanical properties under compressive and tensile strain were measured using universal testing machine (UTS, Lloyd, UK). Other details regarding specimen and used parameters are reported in our previous work [14]. Hardness of the composite was determined by using Westop durometer according to ASTM D 2583 standards. Finally, the energy harvesting measurements were performed using a cyclic testing machine (Samick-THK, South Korea).

3. Results and discussion

3.1. Morphology and particle size of TiO_2

The particle size and surface area of the TiO_2 demonstrated a significant effect on the properties of rubber composites. Therefore, we measured the particle size and BET surface area of TiO_2 particles to analyse their effect on mechanical and energy harvesting properties. Fig. 1 shows the SEM images of different TiO_2 particles depicting morphology and particle sizes.

In Fig. 1(Ia), TiO_2 particles show an average size of ~147 nm and are used as microfiller. In contrast, the size dimensions of other TiO_2 particles in Fig. 1 (Ib and Ic) are used as nanofillers (i.e. ~34 nm and ~29 nm), respectively. Fig. 1-II provides the schematic illustration of the fabrication of RTV-SR/TiO_2 NPs composites.

3.2. Adsorption-desorption isotherms and X-ray diffraction for the nanofillers

The adsorption-desorption isotherms of nanofillers was performed to estimate their BET surface area (Fig. 2a-c).

The measurements found that the different grades of TiO_2 were 3 m^2/g, 50 m^2/g, and 145 m^2/g. The volume of gas adsorbed enhanced as the BET surface was increased. Here, it can be described that the surface area is directly correlated with adsorbed gas by the particles [27]. Moreover, the adsorption isotherms can also provide other characteristics of filler, such as surface activity, BET surface area, and porosity, as described elsewhere [27]. Herein, it is interesting to note that the slope in Fig. 2c is different from those of Fig. 2a-b. It is speculated that the hysteresis present between the adsorption and desorption curves in Fig. 2c could be due to the mesoporous

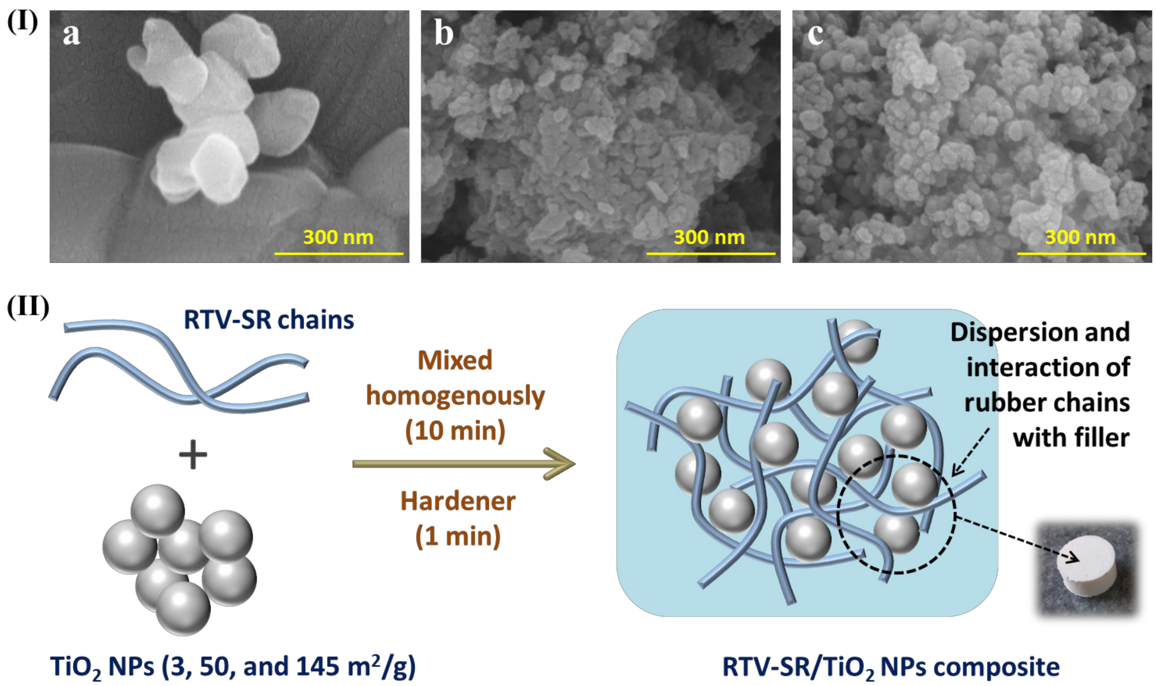

Figure 1. **(I)** (a) SEM images of various types of TiO_2 as filler particles and **(II)** a schematic illustration of the fabrication of RTV-SR/TiO_2 composites.

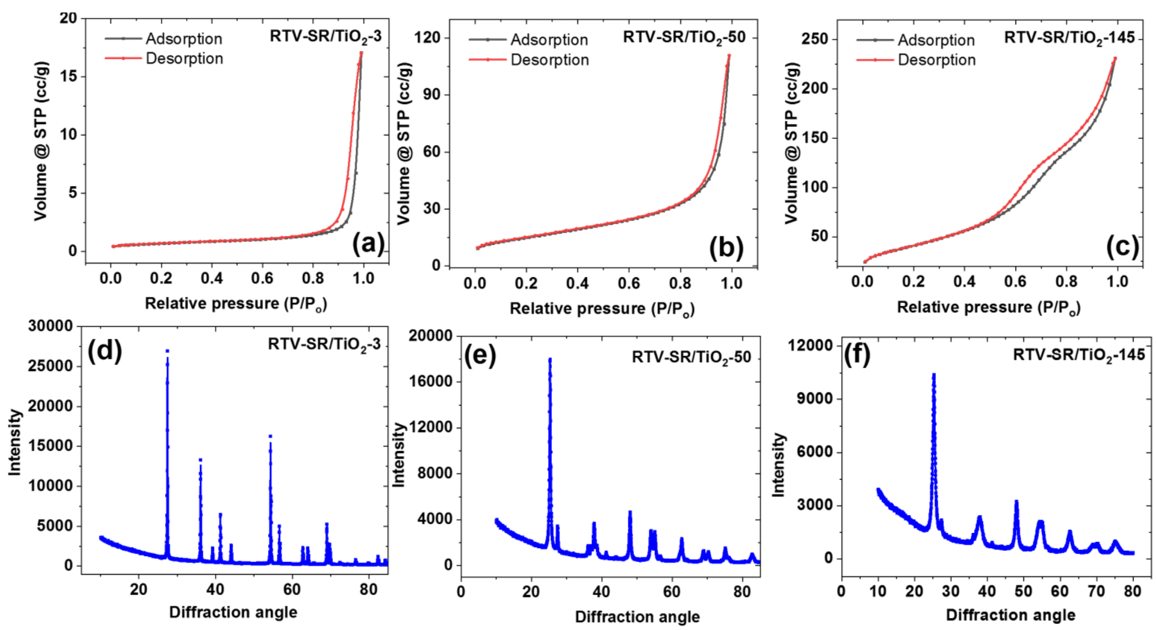

Figure 2. Adsorption-desorption isotherms **(a-c)** and XRD patterns **(d-f)** of various types of TiO_2 NPs.

filling and emptying processes that occur at a higher relative pressure (> ~ 0.4). Another possible reason could be the formation of pseudo pores due to aggregation/clumping of particles in the material, which may result in a hysteresis loop formation. The crystal structure of the fillers was determined by XRD analysis (Fig. 2d-f). The XRD patterns of different types of TiO_2 show their highly crystalline structure [14]. Further, the peak intensity was found to decrease as a function of the density distribution of the nanoparticles. As witnessed from SEM images in Fig. 1a-c, the density and number of particles were changed with changing in the surface area and particle sizes. Therefore, there is a direct correlation of peak intensities with the type of TiO_2 particle which is investigated.

3.3. Properties of RTV-SR/TiO_2 composites

3.3.1. Filler dispersion using optical microscopy

The filler dispersion plays a determining role in affecting the properties of the composites [28]. In the present work, optical microscopy determines the filler dispersion in the rubber matrix.

The optical micrographs of different composites are shown in Fig. 3. The surface morphology of the virgin sample (non-reinforced RTV-SR) is devoid of the filler (Fig. 3a), while in Fig. 3b, RTV-SR/TiO_2-3 composite shows good dispersion of TiO_2 particles in the RTV-SR matrix. Here, the micron size of the TiO_2 particles was used in composite preparation with a low surface area of 3 m^2/g. However, the particle size of the remaining composites was small, with a high surface area in the range of 50 m^2/g (Fig. 3c) or 145 m^2/g (Fig. 3d). Therefore, optical micrographs of the composites show improved dispersion (Fig. 3c and 3d) compared to the sample, shown in Fig. 3b.

Furthermore, filler-rich zones with TiO_2 particles in the RTV-SR matrix were also evidenced. These features justify the higher properties of composites with nano-size TiO_2 particles. Moreover, the homogenous dispersion of nano-sized TiO_2 particles into the rubber matrix facilitates the improvement in the composite's mechanical properties and leads to the high performance of energy harvesting device.

3.3.2. Filler dispersion using Elemental mapping

As the filler dispersion in the matrix has a significant effect on the final properties, the dispersion of TiO_2 particles was also estimated by elemental mapping (SEM/EDX) (see Fig. 4, as

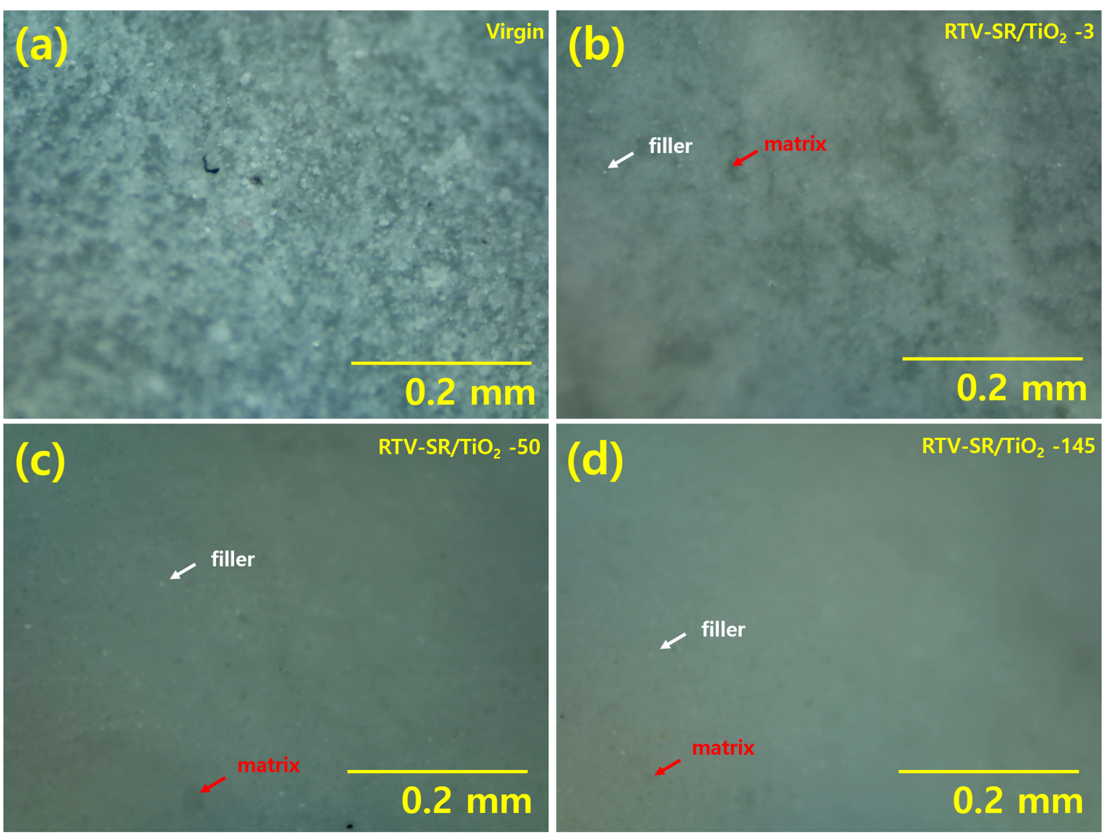

Figure 3. Filler dispersion of TiO_2 particles through optical microscopy of different composites **(a-d)** at 150x.

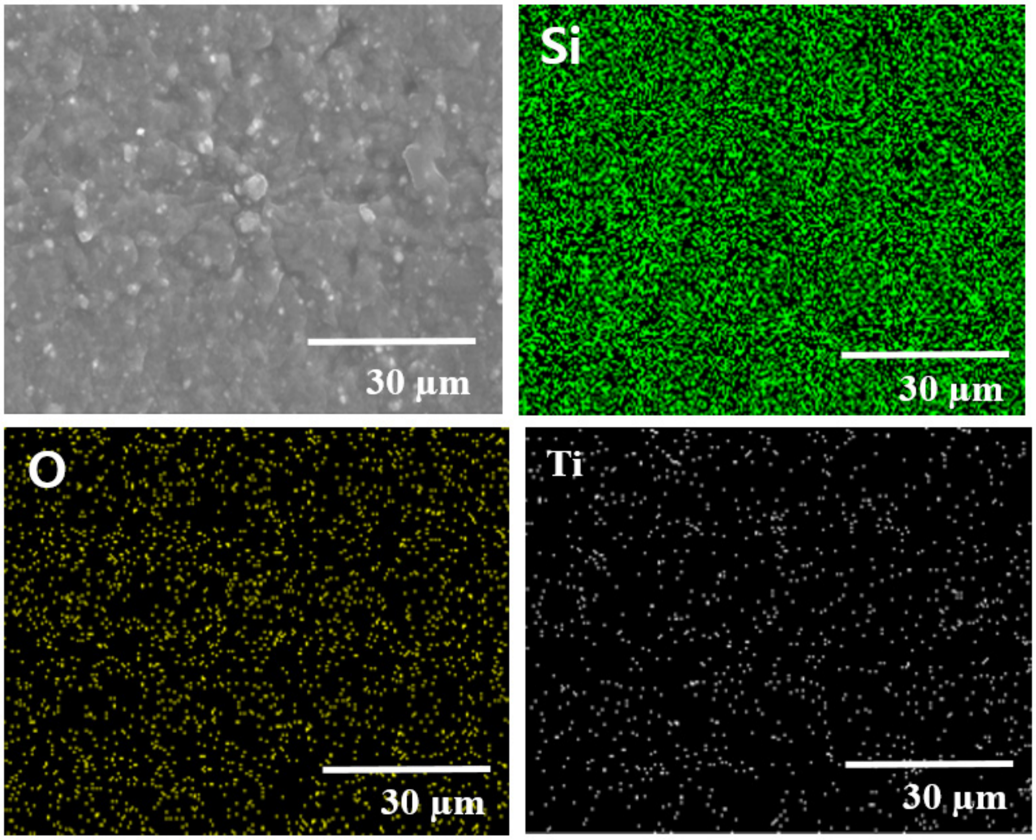

Figure 4. Filler dispersion detected by elemental mapping of 6 phr of RTV-SR/TiO_2-145 composite [14].

reported in our previous study) in addition to the optical microscopical analysis.

The Si element was noted to be originated from virgin RTV-SR, and the O and Ti elements were known to be originated from TiO_2 filler [14]. From the elemental mapping, it can be noted that the Ti and O elements were homogenously distributed throughout the rubber matrix. Also, the measurements further justify the absence of percolative networks as noted from Ti and O elemental mappings. Moreover, no signatures of aggregation among the filler particles were detected from the elemental mappings.

3.4. Mechanical properties

Mechanical properties strongly depend on the particle size or BET surface area of the filler used in reinforcing rubber matrix [28]. The filler with a small particle size and high surface area are known to exhibit high mechanical properties even at lower filler amount in the rubber composite. Moreover, the mechanical behavior was known to be different under different types of strain, such as compressive or tensile strains. The mechanical properties under compressive strain were studied and are shown in Fig. 5 (a and b). In Fig. 5a, it was found that the compressive stress was increased with increasing compressive strain from 0 to 35% at maximum. Such an increase under compressive strain is due to an increase in the packing fraction of filler and polymer chains of rubber in composites [29]. Moreover, the compressive stress increased with increasing TiO_2 particles upto 6 phr and then decreased. This increase in compressive stress up to 6 phr is due to improved interfacial area and interactions, improved filler networking and high stress transfer at the filler-polymer interface [30]. The fall in mechanical properties after 6 phr is due to aggregation of TiO_2 particles in the rubber matrix. The effect is possibly due to the difficulty in achieving a homogenous dispersion of nanoparticles in the polymer matrix owing to their strong agglomeration tendency. Therefore, the mechanical properties (e.g., Young's modulus) decreased when the filler content (i.e. TiO_2) was

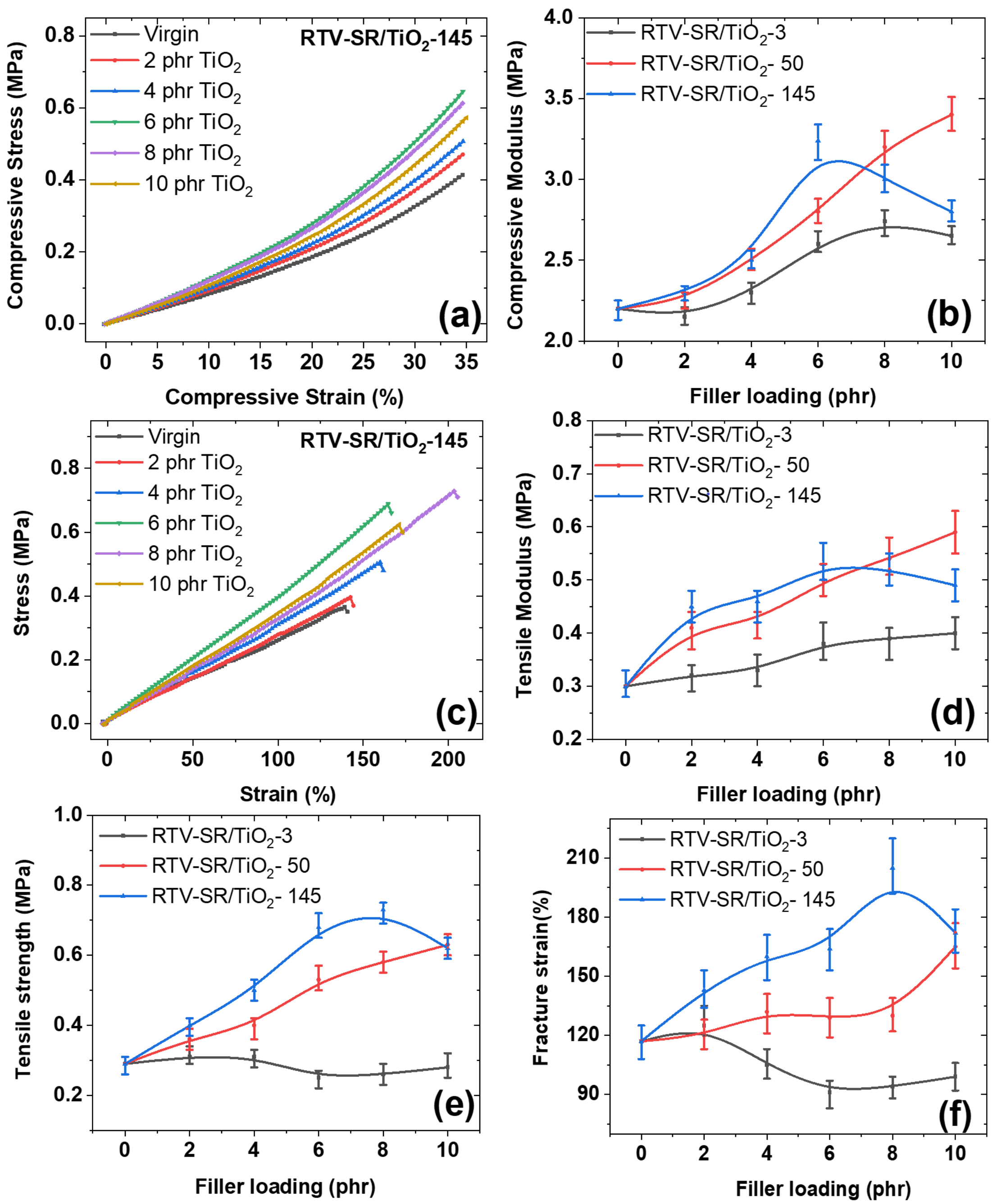

Figure 5. Compressive mechanical properties; **(a)** compressive stress-strain of RTV-SR/TiO_2-145 sample; **(b)** compressive modulus of different types of samples. Tensile mechanical properties; **(c)** profiles of tensile stress as a function of tensile strain; **(d)** Tensile modulus for different fillers; **(e)** tensile strength of the composites; **(f)** fracture strain for different composites.

greater than 6 phr. In the case of RTV-SR/TiO_2-145, the smaller size of TiO_2 particles allows for a higher surface area to be available for matrix/filler interaction and thereby more chances for agglomeration of particles at higher content as compared to RTV-SR/TiO_2-50.

The behavior of compressive modulus was also measured for different types of TiO_2 particles in the RTV-SR matrix (Fig. 5b).

It was found that the TiO_2 particles with high surface area and small particle size was found to promote higher compressive modulus, while the TiO_2 particles with micro-particle size and low surface area showed lower compressive modulus [31]. Therefore, the nano-effect of TiO_2 particles was observed, and higher improvement in mechanical properties was noticed. Notably, filler with higher surface area exhibited higher compressive modulus due to improved interfacial interactions. Filler is known to exhibit higher surface energy. Due to this property, polymer chains (rubber) with lower surface energy are adsorbed on the surface of filler and cause mechanical reinforcement. Thus, the filler with a higher surface area and small particle size promote higher compressive mechanical properties.

The tensile mechanical properties such as tensile modulus, tensile strength and fracture strain were estimated and demonstrated in Fig. 5(c-e). It was found from Fig. 5c that the tensile stress increased with increasing tensile strain until fracture. It is noticeably due to enhanced filler networking and improved interfacial interaction between filler and polymer chains of rubber matrix [32]. Moreover, with increasing content of TiO_2 particles, the tensile stress increased up to 8 phr and then it was decreased. Further, the fall in tensile strain after 8 phr is due to aggregation of TiO_2 particles in the rubber matrix.

In Fig. 5d, the tensile modulus was measured as a function of TiO_2 particles loading in the RTV-SR matrix. It was found that the tensile modulus increased as a function of TiO_2 particles content for all composites, except RTV-SR/TiO_2-145 specimen, where it falls after 6 phr. The higher tensile strength for TiO_2 particles with small particle size and higher surface area is due to improved filler networking and nano-size filler dispersion. Moreover, the fall in properties of RTV-SR/TiO_2-145 specimen is due to the possible aggregation of filler particles in the rubber matrix. Fig. 5e and 5f present the tensile strength and the fracture strain behavior of the composites. Here, it was found that the tensile strength and fracture strain were higher for RTV-SR/TiO_2 composites with small particle sizes and high surface area. The improved properties for a higher surface area of TiO_2 particles were due to improved filler networking and higher interfacial area for excessive polymer chains of rubber matrix to interact with the filler surface [33]. The fall in fracture strain and tensile strength of RTV-SR/

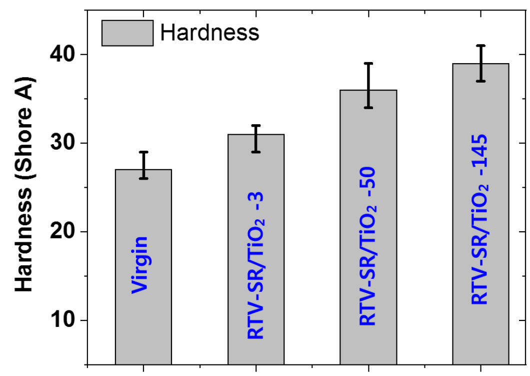

Figure 6. Hardness of different composites at 6 phr of TiO_2 particles in RTV-SR matrix.

TiO_2-145 after 8 phr is due to aggregation of filler particles in the rubber matrix. The poor tensile strength and fracture strain of RTV-SR/TiO_2-3 specimen is due to micron size particles and poor interfacial area, where fewer polymer chains are available to interact with filler surface and thereby a poor stress-transfer from rubber to filler. It is interesting to note that all the samples show no signatures of plastic deformation once the stress is removed.

Hardness is a mechanical property that provides key evidence of composites, whether hard or soft. The composites with a hardness below 65 are classified as soft composites [15]. Fig. 6 justifies that the composites show hardness very far below65 and thus are classified as soft composites. These soft composites are useful for various applications such as flexible devices and high-performance energy harvesting devices [34]. It was also found that the hardness was co-related with surface area and particle size of TiO_2 particles. The composites reinforced with higher surface area and smaller particle size of TiO_2 particles showed higher hardness values (Fig. 6). The higher hardness for high surface area filler is due to improved filler dispersion, higher interfacial area that promotes high interfacial interaction and improved stress transfer from strained polymer chains to TiO_2 particles.

3.5. Energy harvesting

The flexible energy harvesting device based on rubber composites can provide continuous voltage against the mechanical strains [35].

These dielectric elastomers-based energy harvesting devices undergo mechanical strains

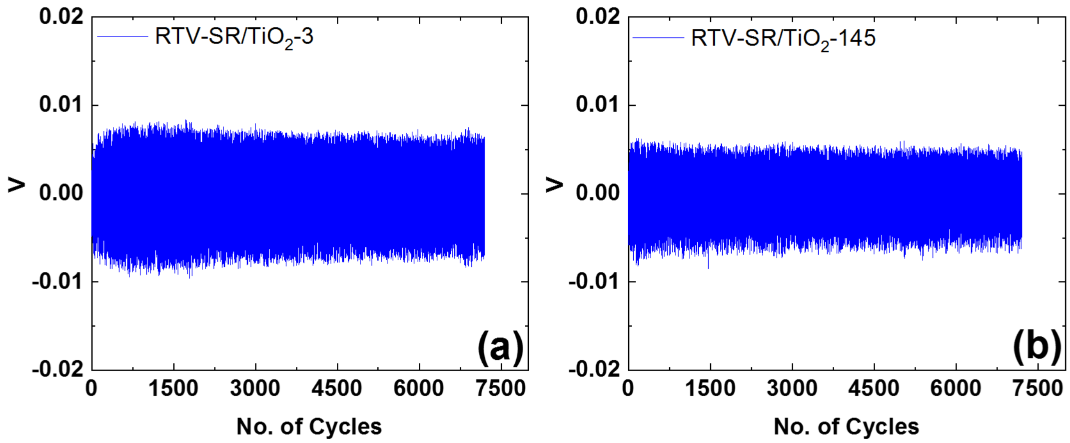

Figure 7. Energy harvesting for the composites at 6 phr of TiO_2 particles: **(a)** RTV-SR/TiO_2-3 and **(b)** RTV-SR/TiO_2-145.

or mechanical motions and produce voltage [36]. Here, the energy is harvested using an elastomer substrate based on dielectric RTV-SR rubber and an electrode based on different types of TiO_2 (Fig. 7). It was found that the output voltage generation was in few millivolts for two kinds of electrodes and the type of TiO_2 did not influence the output voltage significantly. It was also evidenced that both devices' output voltage was stable for up to 7500 cycles. It indicates that the devices and their respective voltage generation are least deformed in respect of an increased number of cycles, and therefore they demonstrated high durability.

3.6. Figure of Merit

The Figure of merit summarizes the results on mechanical properties and output voltage based on the influence of the surface area and particle size.

For the mechanical behavior of the composites in Fig. 8 (a-c), an increase in surface area and decrease in particle size exhibited the increased compressive modulus, tensile strength, and fracture strain. Such an increase in mechanical properties is due to improved filler networking and the so-called nano-effect of the filler. The nanofiller provided high interfacial interaction and resulted in high mechanical properties of the composites. However, the output voltage in the energy harvesting device was not influenced by the surface area of fillers (Fig. 8d). Since the voltage generation is influenced by electrode electrical conductivity, the conductivity of the composites seems to be influenced significantly by TiO_2 particles, particularly with reduced particle sizes.

4. Conclusion

The composites were successfully prepared by mixing different types of TiO_2 particles and the RTV-SR matrix. In this study, the adsorption-desorption measurement was performed to analyse the BET surface area of different TiO_2 particles as 3 m^2/g, 50 m^2/g, and 145 m^2/g for different particle sizes of TiO_2 as 147 nm, 34 nm, and 29 nm, respectively, wherein a correlation between particle size and BET surface area has been established. By taking these TiO_2 particles, the flexible RTV-SR/TiO_2 electrodes were fabricated by incorporating TiO_2 particles with different surface areas and sizes in the RTV-SR as a flexible substrate for energy generation. Herein, we demonstrate the effect of the surface area of TiO_2 on mechanical properties and energy harvesting efficiency. Optical micrographs showed the homogenous dispersion of TiO_2 particles in RTV-SR composites, from micro-size dispersion (low surface area) to nano-size distribution (high surface area) of the TiO_2 particles. In addition, nano-sized TiO_2 particles with higher surface area exhibited higher mechanical properties (e.g., strength and modulus). Moreover, energy harvesting measures demonstrated that the energy harvesting performance was obtained minimally and was not affected significantly by using TiO_2 particles with different sizes or

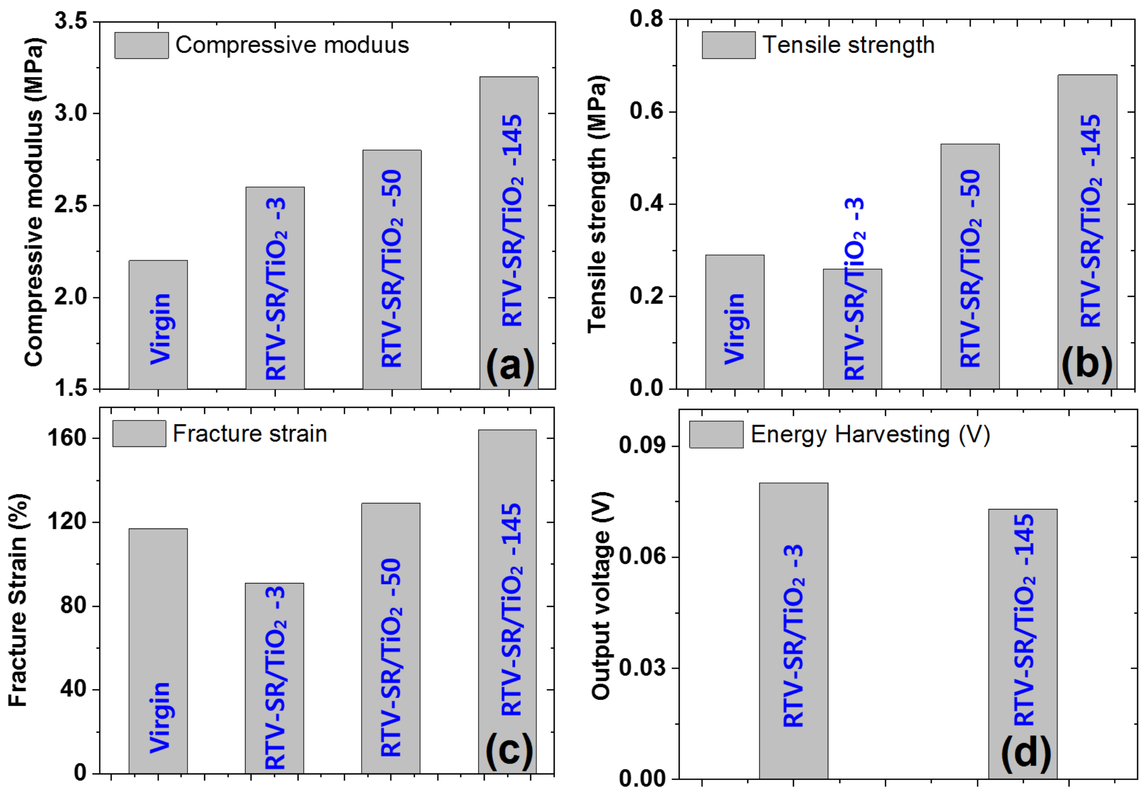

Figure 8. Figure of merit with the summary of mechanical properties of different composites at 6 phr of TiO_2 particles with different surface area and particle size: **(a)** compressive modulus, **(b)** tensile strength, **(c)** fracture strain, and **(d)** output voltage in energy harvesting device.

surface areas. From the figure of merit, it is clear that the surface area and particle size of TiO_2 play an essential role in determining the mechanical properties of composites. Therefore, utilising TiO_2 particles with high surface area is promising to obtain high mechanical properties of composites. Additionally, the RTV-SR/TiO_2 composites exhibited hardness values (Shore A) below 65, which are highly anticipated for use in soft composite applications (e.g., soft actuation and flexible soft energy harvesting). Moreover, the RTV-SR/TiO_2 composites may have potential applications for flexible electronics.

Acknowledgements

The research work was supported by the NRF fund (2017R1D1A3B03031732) by the Ministry of Education, Republic of Korea.

References

[1] Van den Ende DA, Van de Wiel HJ et al. Direct strain energy harvesting in automobile tires using piezoelectric PZT–polymer composites, Smart Materials and Structure. 2011; 21(1): 015011.

[2] Taghavi M, Mattoli V, Sadeghi A et al. A Novel Soft Metal-Polymer Composite for Multidirectional Pressure Energy Harvesting, Advanced Energy Materials, 2014; 4(12):1400024.

[3] Xiao TX, Jiang T, Zhu JX, Liang X, Xu L et al. Silicone-based triboelectric nanogenerator for water wave energy harvesting, ACS Applied Materials & Interfaces, 2018, 10(4):3616–23.

[4] Wang C, Zhao J, Li Q, Li Y et al. Optimization design and experimental investigation of piezoelectric energy harvesting devices for pavement, Applied Energy, 2018, 229:18-30.

[5] Liu D, Song L, Song H, Chen J, Tian Q, Chen L et al. Correlation between mechanical properties and microscopic structures of an optimized silica fraction in silicone rubber, Composite Science and Technology, 2018, 165:373-379.

[6] Bueche AM, Filler reinforcement of silicone rubber, Journal of Polymer Science, 1957, 25(109):139-49.
[7] Zhou W, Qi S, Tu C, Zhao H, Wang C et al. Effect of the particle size of Al_2O_3 on the properties of filled heat-conductive silicone rubber, Journal of Polymer Science, 2007, 104(2): 1312-18.
[8] Demjén Z, Pukánszky B, Nagy J et al. Evaluation of interfacial interaction in polypropylene/surface treated $CaCO_3$ composites, Composites Part A: Applied Science and Manufacturing, 1998, 29(3): 323-29.
[9] Namitha LK, Chameswary J, Ananthakumar S et al. Effect of micro-and nano-fillers on the properties of silicone rubber-alumina flexible microwave substrate, Ceramics International, 2013, 39(6): 7077-87.
[10] Abbasipour M, Khajavi R, Yousefi AA et al. Improving piezoelectric and pyroelectric properties of electrospun PVDF nanofibers using nanofillers for energy harvesting application, Polymer for Advanced Technology, 2019, 30(2):279-91.
[11] Datta J, Kosiorek P, Włoch M, Effect of high loading of titanium dioxide particles on the morphology, mechanical and thermo-mechanical properties of the natural rubber-based composites, Iranian Polymer Journal, 2016, 25:1021–35.
[12] Ponnamma D, Sadasivuni KK, Strankowski M, Guo Q et al. Synergistic effect of multi walled carbon nanotubes and reduced graphene oxides in natural rubber for sensing application, Soft Matter, 2013, 9:10343-53.
[13] Kumar V, Kumar A, Han SS, Park SS, RTV silicone rubber composites reinforced with carbon nanotubes, titanium-di-oxide and their hybrid: Mechanical and piezoelectric actuation performance, Nano Materials Science, 2021, 3(3):233-40.
[14] Kumar V, Kumar A, Song M, Lee DJ, Han SS, Park SS, Properties of Silicone Rubber-Based Composites Reinforced with Few-Layer Graphene and Iron Oxide or Titanium Dioxide, Polymers, 2021, 13(10):1550.
[15] Wang YX, Wu YP, Li WJ, Zhang LQ, Influence of filler type on wet skid resistance of SSBR/BR composites: Effects from roughness and micro-hardness of rubber surface, Applied Surface Science, 2011, 257(6):2058-65.
[16] El-Hag AH, Jayaram SH et al. Fundamental and low frequency harmonic components of leakage current as a diagnostic tool to study aging of RTV and HTV silicone rubber in salt-fog, IEEE Transactions on Dielectrics and Electrical Insulation, 2003, 10(1):128-36.
[17] Polmanteer KE, Current perspectives on silicone rubber technology, Rubber Chemistry and Technology, 1981, 54(5):1051–80.
[18] Kumar V, Alam MN, Manikkavel A, Song M, Lee DJ et al. Silicone rubber composites reinforced by carbon nanofillers and their hybrids for various applications: A review, Polymers, 2021, 13(14):2322.
[19] Boccalero G, Jean-Mistral C, Castellano M et al. Soft, hyper-elastic and highly-stable silicone-organo-clay dielectric elastomer for energy harvesting and actuation applications, Composites Part B: Engineering, 2018, 146:13-19.
[20] Yang X, Li Z, Jiang Z, Wang S, Liu H, Xu X, Wang D et al. Mechanical reinforcement of room-temperature-vulcanized silicone rubber using modified cellulose nanocrystals as cross-linker and nanofiller, Carbohydrate Polymers, 2020, 229:115509.
[21] Yang X, Jiang Z, Liu H, Zhang H, Xu X, Shang S et al. Performance improvement of rosin-based room temperature vulcanized silicone rubber using nanofiller fumed silica, Polymer Degradation and Stability, 2021, 183:109422.
[22] Zhao J, Zhang J, Wang L, Lyu S, Ye W, Xu BB et al. Fabrication and investigation on ternary heterogeneous MWCNT@ TiO_2-C fillers and their silicone rubber wave-absorbing composites, Composites Part A: Applied Science and Manufacturing, 2020, 129:105714.
[23] Islamipour, Z, Zare, EN, Salimi, F, Ghomi, M, Makvandi, P. Biodegradable antibacterial and antioxidant nanocomposite films based on dextrin for bioactive food packaging, Journal of Nanostructure in Chemistry, 2022: 1-16.
[24] Zare, EN, Zheng, X, Makvandi, P, Gheybi, H, Sartorius, R, Yiu, CK et al. Nonspherical Metal-Based Nanoarchitectures: Synthesis

and Impact of Size, Shape, and Composition on Their Biological Activity. Small, 2021, 17(17): 2007073.
[25] Kumar V, Kumar A, Alam MN, Park SS, Effect of graphite nanoplatelets surface area on mechanical properties of room-temperature vulcanized silicone rubber nanocomposites, Journal of Applied Polymer Science, 2022, e52503, https://doi.org/10.1002/app.52503.
[26] Kumar V, Park SJ, Lee DJ, Park SS, Mechanical and magnetic response of magneto-rheological elastomers with different types of fillers and their hybrids, Journal of Applied Polymer Science, 2021, 138(37):50957.
[27] Möwes MM, Fleck F, Klüppel M, Effect of filler surface activity and morphology on mechanical and dielectric properties of NBR/Graphene nanocomposites, Rubber Chemistry and Technology, 2014, 87(1):70–85.
[28] Alter H, Filler particle size and mechanical properties of polymers, Journal of Applied Polymer Science, 1965, 9(4):1525-31.
[29] Hall LM, Anderson BJ, Zukoski CF et al. Concentration fluctuations, local order, and the collective structure of polymer nanocomposites, Macromolecules, 2009, 42(21):8435–42.
[30] Jayaraman A, Schweizer KS, Effective interactions, structure, and phase behavior of lightly tethered nanoparticles in polymer melts, Macromolecules, 2008, 41(23): 9430–8.
[31] Zhou Y, White E, Hosur M, Jeelani S et al. Effect of particle size and weight fraction on the flexural strength and failure mode of TiO_2 particles reinforced epoxy, Materials Letters, 2010, 64(7):806-9.
[32] Che J, Wu K, Lin Y, Wang K, Fu Q, Largely improved thermal conductivity of HDPE/expanded graphite/carbon nanotubes ternary composites via filler network-network synergy, Composites Part A: Applied Science and Manufacturing, 2017, 99:32-40.
[33] Zhou H, Deng H, Zhang L, Fu Q, Significant enhancement of thermal conductivity in polymer composite via constructing macroscopic segregated filler networks, ACS Applied Materials & Interfaces, 2017, 9(34): 29071–81.
[34] Peddigari M, Kim GY, Park CH, Min Y, Kim JW, Ahn CW et al. A comparison study of fatigue behavior of hard and soft piezoelectric single crystal macro-fiber composites for vibration energy harvesting, Sensors, 2019, 19(9):2196.
[35] Gao D, Liu C, Fan S, A new type of flexible energy harvesting device working with micro water droplets achieving high output, Journal of Materials Chemistry A, 2021, 9:23555-62.
[36] Kornbluh RD, Pelrine R, Prahlad H, Wong-Foy A et al. Dielectric elastomers: Stretching the capabilities of energy harvesting, MRS Bulletin, 2012, 37(3):246-53.